Supporting Information for:

In-situ-binding Sb Nanospheres on Graphene via Oxygen Bonds as Superior Anode for Ultrafast Sodium Ion Batteries

Fang Wan,[a] Jin-Zhi Guo,[a] Xiao-Hua Zhang,[a] Jing-Ping Zhang,[a] Hai-Zhu Sun,[a] QingYu Yan,[b] Dong-Xue Han,[c] Li Niu,[c] and Xing-Long Wu[ab]*

[a] National & Local United Engineering Lab for Power Battery, Faculty of Chemistry, Northeast Normal University, Changchun, Jilin 130024, P. R. China.

[b] School of Materials Science and Engineering, Nanyang Technological University, 50 Nanyang Avenue, Singapore 639798, Singapore

[c] State Key Laboratory of Electroanalytical Chemistry, c/o Engineering Laboratory for Modern Analytical Techniques, Changchun Institute of Applied Chemistry, Chinese Academy of Sciences, Changchun, Jilin 130022, P. R. China.

* The corresponding author

Email addresses: xinglong@nenu.edu.cn (X.-L. Wu)

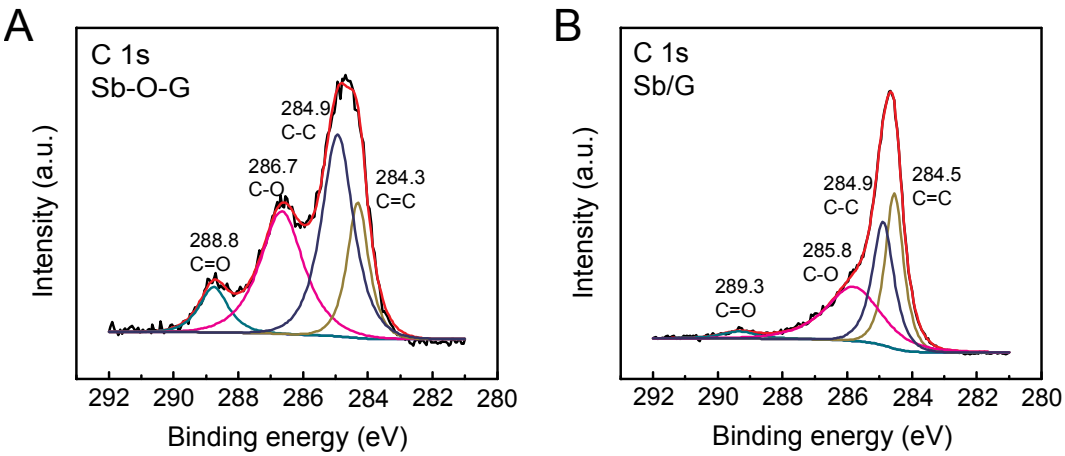

Figure S1. The high-resolution C1s XPS spectra of Sb-O-G (A) and Sb/G (B). From the fitting results, there are four kinds of carbon (C=O, C-O, C-C and C=C) in both materials. However, the Sb-O-G micro/nanomaterial exhibits much higher intensities of carbon atoms connected with oxygen functionalities (C=O and C-O) in comparison with the Sb/G. This make sense since the Ar/H_2 thermal treatment reduced the surface of SbO_x and of rGO.

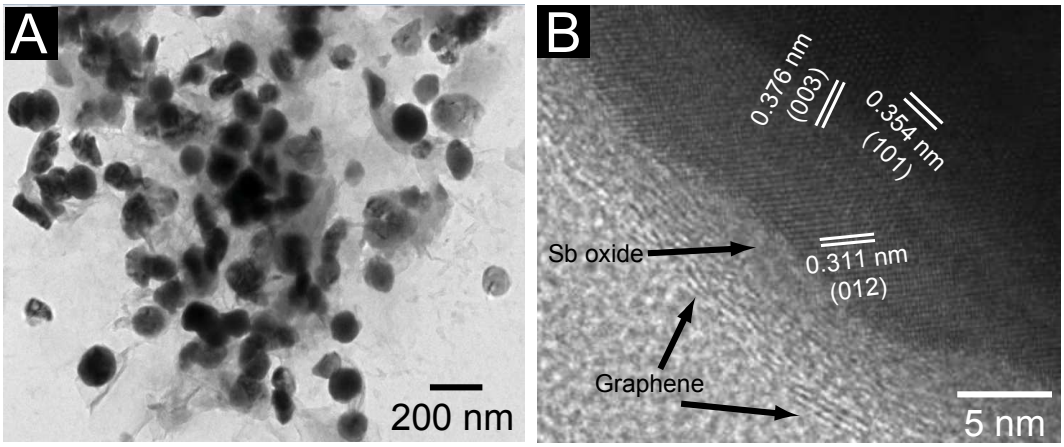

Figure S2. TEM (A) and high-resolution TEM (B) images of the Sb-O-G micro/nanomaterial. It is clearly seen from Figure S2A that the Sb nanospheres of about 100 nm are well wrapped by the rGO nanosheets. And as shown in HRTEM (Figure S2B), the (003), (101) and (012) lattice planes are discovered. Moreover, there is a thin Sb oxide layer between Sb and graphene.

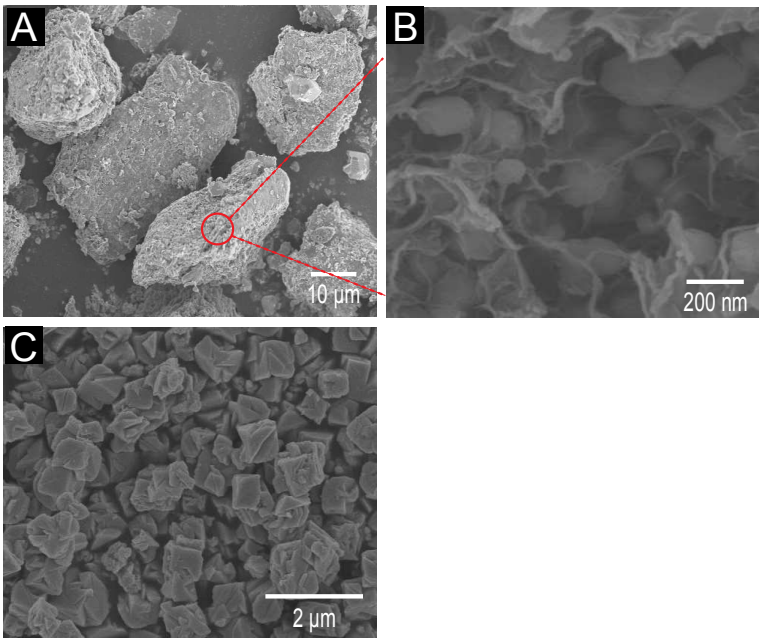

Figure S3. SEM images of Sb/G composite (A, B) and pure Sb material (C).

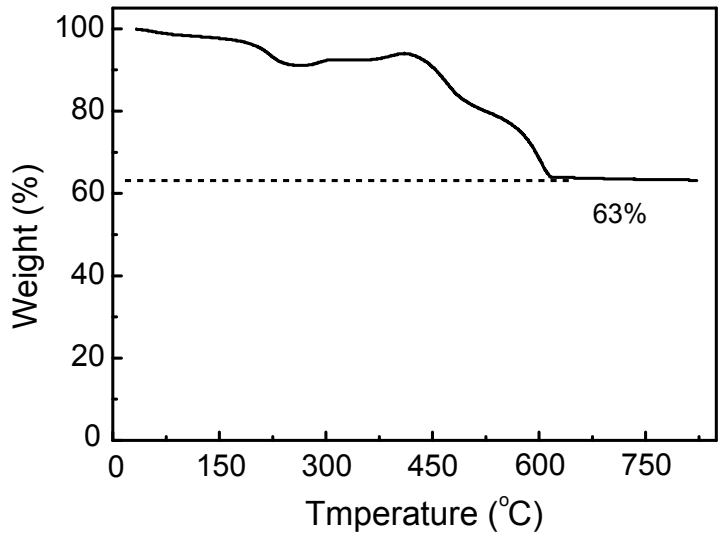

Figure S4. The thermal gravimetric analysis (TGA) curve of Sb-O-G micro/nanomaterial under air atmosphere at a heating rate of 10 ^{o}C/min. It is calculated for TGA that the contents of Sb and rGO components are 53 % and 47% respectively.

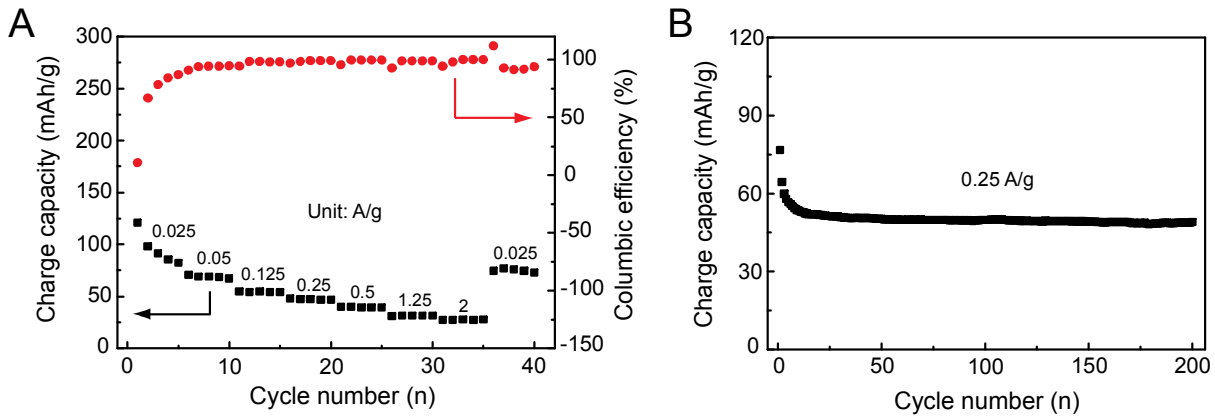

Figure S5. The Na-storage properties of pure rGO material: (A) rate capabilities at the current densities from 0.025 to 2 A/g, and (B) cycling performance at 0.25 A/g. The rGO electrodes were composed of 80% rGO, 10% acetylene black and 10% polyvinylidene fluoride.

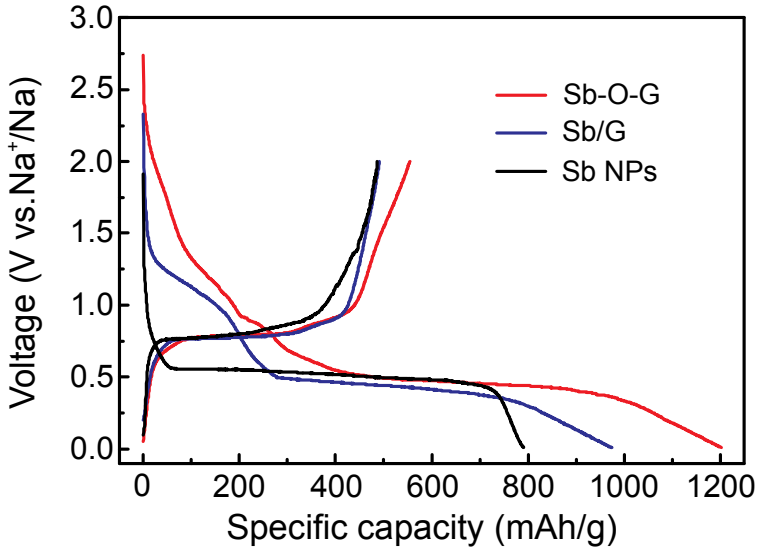

Figure S6. The comparison of initial 1st charge-diacharge curves of pure Sb NPs, Sb/G and Sb-O-G micro/nanomaterials in half cells. The current density is 25 mA/g.

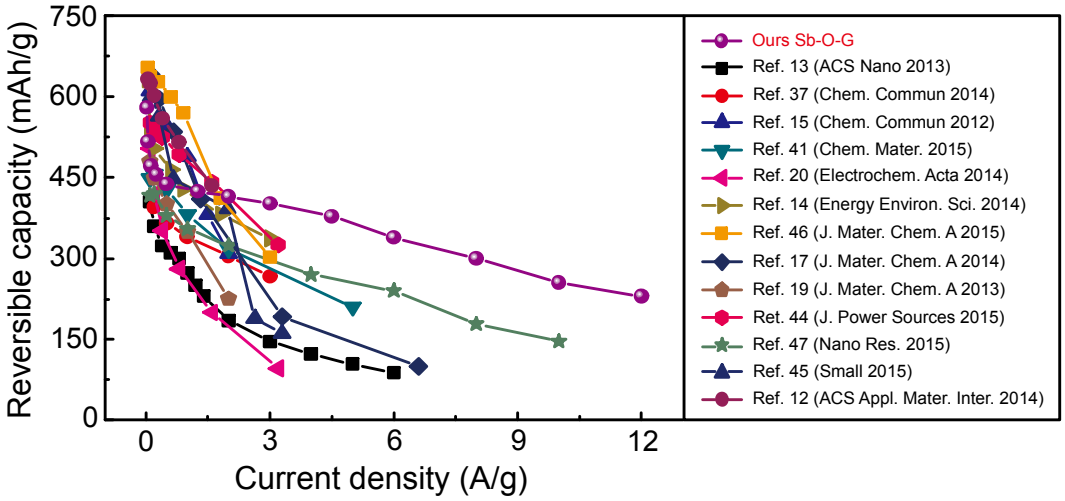

Figure S7. The comparison of rate performances of Sb-O-G and previous reports.

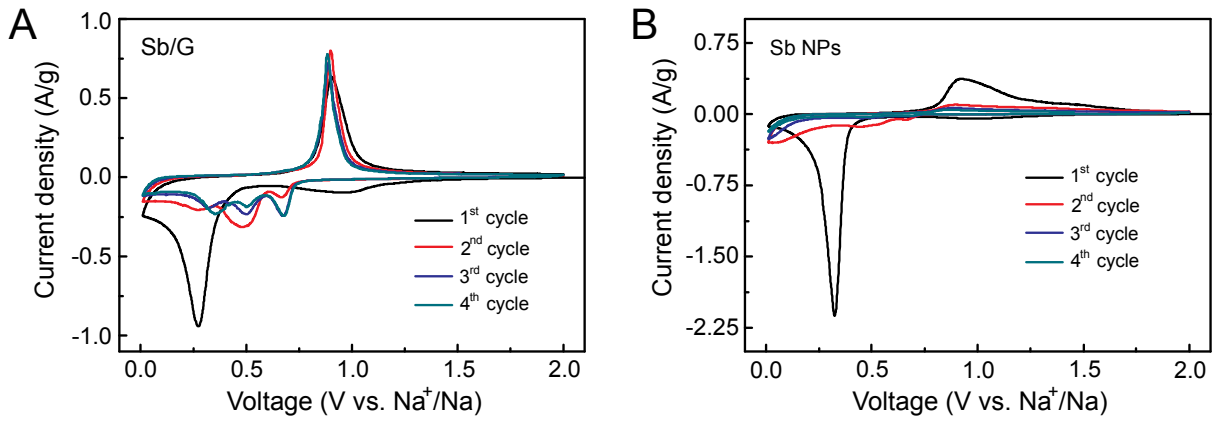

Figure S8. The CV patterns of Sb/G (A) and Sb NPs (B) at a scanning rate of 0.1 mV/s in the voltage range from 0.01 V to 2 V. The tests were implemented in half cells with metallic Na as both counter and reference electrodes.

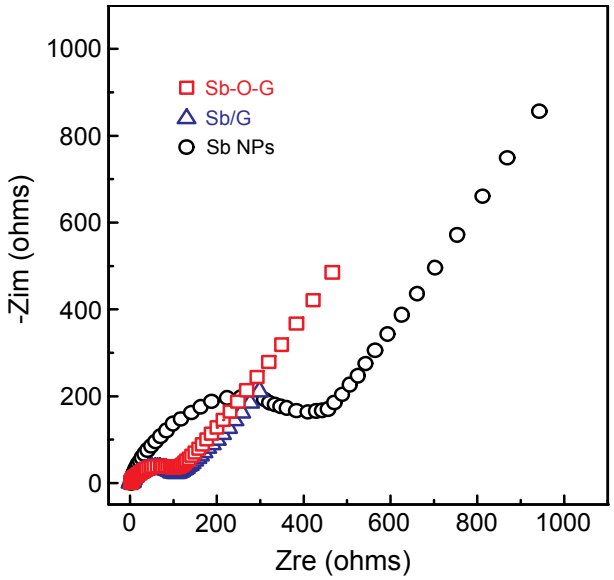

Figure S9. The comparison of EIS Nyquist plots between the electrodes of pure Sb NPs, Sb/G and Sb-O-G micro/nanomaterials. Note that, the EIS tests were carried out on the half cells after one discharge/charge cycle.

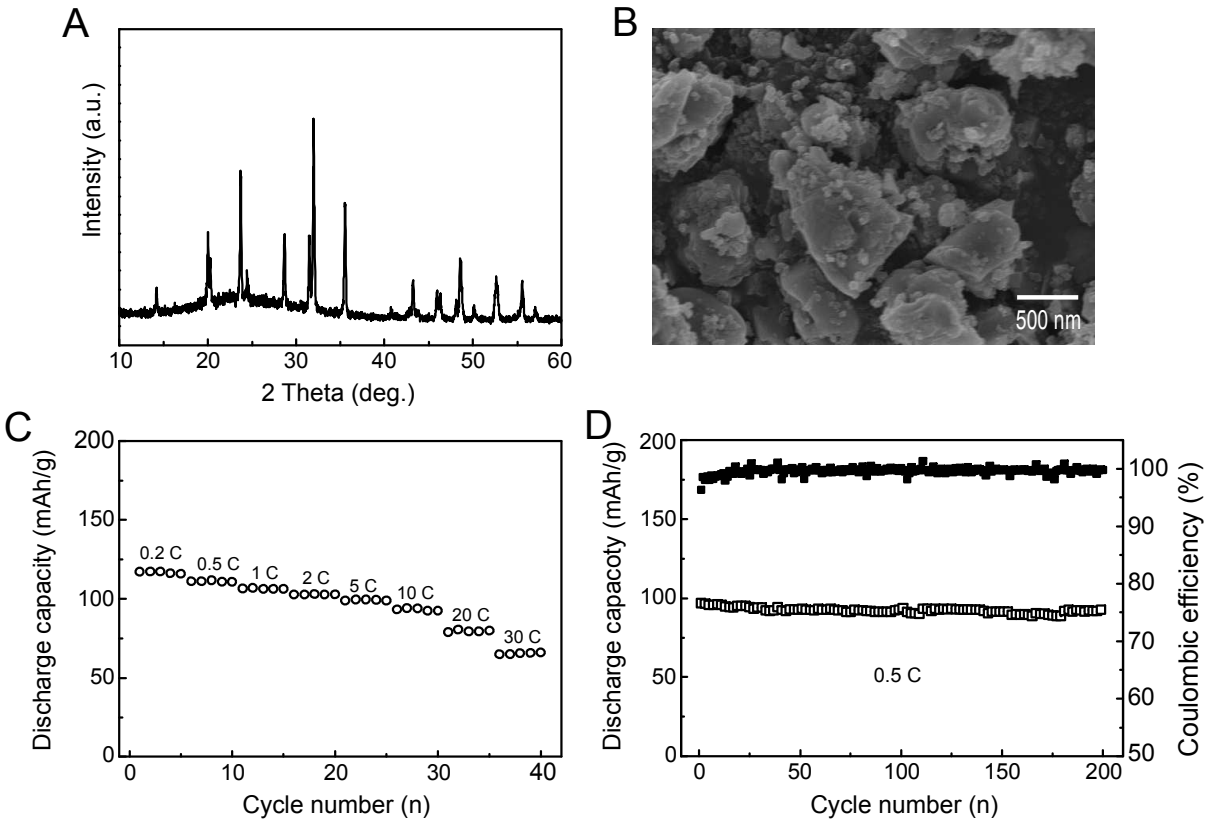

Figure S10. XRD pattern (A), SEM image (B), rate capabilities (C) and cycling performance (D) of the prepared $Na_3V_2(PO_4)_3$ material used as cathode for full-cell evaluation.